Clonal precursor of bone, cartilage, and hematopoietic niche stromal cells

Charles K. F. Chan[a,1,2], Paul Lindau[a,1], Wen Jiang[a,1], James Y. Chen[a,3], Lillian F. Zhang[a,3], Ching-Cheng Chen[b,3,4], Jun Seita[a,3], Debashis Sahoo[a,3], Jae-Beom Kim[b,3,5], Andrew Lee[a], Sujin Park[a], Divya Nag[a], Yongquan Gong[a], Subhash Kulkarni[a], Cynthia A. Luppen[b,6], Alexander A. Theologis[a], Derrick C. Wan[a], Anthony DeBoer[a], Eun Young Seo[a], Justin D. Vincent-Tompkins[a], Kyle Loh[a], Graham G. Walmsley[a], Daniel L. Kraft[a], Joseph C. Wu[a], Michael T. Longaker[a,2,7], and Irving L. Weissman[b,2,7]

[a]Department of Surgery, H3680, Stanford University School of Medicine, Stanford, CA 94305; and [b]Departments of Pathology and Developmental Biology, Institute for Stem Cell Biology and Regenerative Medicine, Stanford University, Palo Alto, CA 94305

Organs are composites of tissue types with diverse developmental origins, and they rely on distinct stem and progenitor cells to meet physiological demands for cellular production and homeostasis. How diverse stem cell activity is coordinated within organs is not well understood. Here we describe a lineage-restricted, self-renewing common skeletal progenitor (bone, cartilage, stromal progenitor; BCSP) isolated from limb bones and bone marrow tissue of fetal, neonatal, and adult mice. The BCSP clonally produces chondrocytes (cartilage-forming) and osteogenic (bone-forming) cells and at least three subsets of stromal cells that exhibit differential expression of cell surface markers, including CD105 (or endoglin), Thy1 [or CD90 (cluster of differentiation 90)], and 6C3 [ENPEP glutamyl aminopeptidase (aminopeptidase A)]. These three stromal subsets exhibit differential capacities to support hematopoietic (blood-forming) stem and progenitor cells. Although the 6C3-expressing subset demonstrates functional stem cell niche activity by maintaining primitive hematopoietic stem cell (HSC) renewal in vitro, the other stromal populations promote HSC differentiation to more committed lines of hematopoiesis, such as the B-cell lineage. Gene expression analysis and microscopic studies further reveal a microenvironment in which CD105-, Thy1-, and 6C3-expressing marrow stroma collaborate to provide cytokine signaling to HSCs and more committed hematopoietic progenitors. As a result, within the context of bone as a blood-forming organ, the BCSP plays a critical role in supporting hematopoiesis through its generation of diverse osteogenic and hematopoietic-promoting stroma, including HSC supportive 6C3(+) niche cells.

endochondral ossification | lymphopoiesis

The postnatal mammalian bone marrow compartment is the site of hematopoiesis and osteogenesis. It consists of cells of osteoid, cartilaginous, and hematopoietic lineages, as well as hematopoietic "niche" cells. This niche, or microenvironment, contains diverse cell types that, with their secreted products, are required by hematopoietic stem cells (HSCs) to generate the full array of blood and immune cells (1, 2). The cellular constitution of niches is poorly understood but is believed to include osteoblasts, endothelial cells, glial cells, vascular pericytes, adipocytes, fibroblasts, and nestin-expressing mesenchymal stromal cells (3–13). The existence of HSC niches is substantiated by evidence that HSCs continuously enter and exit the bone marrow from the peripheral circulation and that direct HSC transplants engraft in numbers that correlate with the number of HSCs in circulation (14, 15).

Although the hematopoietic progenitors and lineages in bone marrow have been isolated and functionally characterized, much less is known about the nonhematopoietic lineages that compose the HSC niche in bone marrow. In this study, we used a reductionist approach to isolating and characterizing the nonhematopoietic cell types that constitute the bone marrow microenvironment (16). Using fluorescent activated cell sorting (FACS), we divided a crude postnatal limb bone and bone marrow suspension from actin–green

fluorescent protein (GFP) mice into distinct fractions. We assessed these fractions by transplanting them under the renal capsule in immunodeficient mice and following their growth. As a result, we identified four functionally distinct fractions: a CD45+ hematopoietic fraction, a CD45-Tie2 (angiopoietin receptor)+alpha V integrin (alphaV)+ population that concurrently generates adipocytes and vessels, a CD45-Tie2-alphaV- fraction that does not appear to produce donor-engrafted tissue, and a CD45-Tie2-alphaV+ population that, through endochondral ossification, forms bone containing robust marrow (Fig. 1 A–D and *SI Appendix,* Fig. S1) (17). In the marrow cavity of these extraskeletal bones, the cells labeled with CD45-Tie2-alphaV+ GFP+ contributed substantially to the stromal compartments (Fig. 1E). When mice harboring these GFP-labeled extraskeletal bones were irradiated and received transplants of red fluorescent protein (RFP) HSCs, the newly transplanted HSCs homed to the GFP-labeled stromal cells in the marrow cavity. This finding indicates that the progenitors of the stromal niche were also contained within the osteoblast and chondrocyte-generating CD45-Tie2-alphaV+ transplanted population (Fig. 1F). CD45-Tie2-alphaV+ cells from bones invariably formed ectopic bones complete with marrow cavities when transplanted into various forms of extraskeletal mesenchymal tissue, including fat, lung, and striated muscle, instead of differentiating into the cell types of their surrounding microenvironment (Fig. 1 G–J and *SI Appendix,* Fig. S2). Unfractionated skeletal stromal cells also formed ectopic bones when transplanted into the heart. These data suggest that tissue progenitors in the bone and bone marrow are predetermined to develop into distinct tissue lineages such as osteoblasts and endothelial cells. Therefore, the specific differentiation capability of each stromal

Fig. 1. Skeletal tissue is composed of lineage restricted tissue progenitors. (*A*) FACS of dissociated bone and bone marrow stroma based on differential expression of CD45, Tie2, and alphaV integrin separates cells into lineage-restricted progenitors of hematopoietic (1), endothelial/adipose (2), and skeletal (3) tissue (FSC-A, forward scatter area; FSC-W, forward scatter width). A fourth population (4) generates only slow growing fibroblastic cells. (*B*) GFP(+) vessels (arrowheads) derived from subcapsular renal transplantation of population 2 in *A* ("a-2") isolated from actin-GFP mice. (Scale bar, 20 μm.) (*C*) GFP(+) adipocytes derived from transplantation of population a-2. (Scale bar, 20 μm.) (*D*) Pentachrome stain of cross-section of ectopic bone derived from transplantation of population a-3. [In pentachrome, red (fibrin) indicates muscle/vascularized tissue; yellow (reticular fibers/collagen) indicates bone; green/blue (mucin) indicates cartilaginous tissue; and black, nuclei and elastic fibers.] (Scale bar, 50 μm.) (*E*) Cross-sectional fluorescence image of ectopic 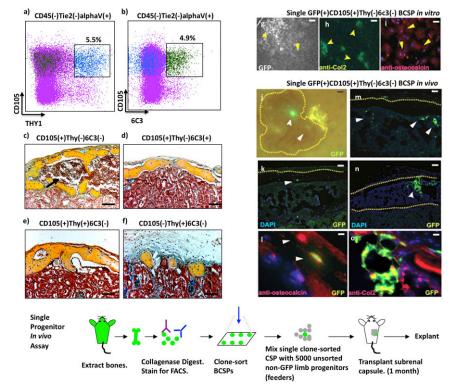bone in *D* showing spongy bone marrow stroma derived from transplantation of population a-3. (Scale bar, 50 μm.) (*F*) An RFP(+)-labeled hematopoietic stem cell (arrowhead) homes to GFP(+) stromal cells in ectopic bone from transplantation of population a-3. (Scale bar, 10 μm.) (*G* and *H*) Bright-field and fluorescent image of ectopic GFP-labeled bone derived from transplant of GFP bone marrow stromal tissue to myocardium. (Scale bar, 1 mm.) (*I* and *J*) Higher-magnification images of *G* and *H*. (Scale bar, 100 μm.) (*K*) Pentachrome stain of cross-section of ectopic bone (yellow dotted circle) in cardiac tissue in *G–J*. (Scale bar, 100 μm.) (*L*) Pentachrome stain of cross-section of femoral head for comparison. (Scale bar, 100 μm.)

subset must be functionally evaluated before clinical use; for instance, in the treatment of cardiac disease (18).

Because the extraskeletal transplantation of the skeletogenic CD45-Tie2-alphaV+ progenitor population generated multiple lineages (including cartilaginous, stromal, and osteoid), we screened additional surface markers by FACS to determine whether the subpopulations within this stromal fraction are separate or linked tissue lineages (19). FACS analysis of mouse limb progenitors at

Fig. 2. CD105, Thy1, and 6C3 label distinct osteogenic populations that are clonally derived from a single CD105(+)Thy(−)6C3(+) common skeletal progenitor. (*A* and *B*) FACS analysis of CD45(−)Tie2(−)alphaV(+) skeletal cells indicating differential expression of CD105 versus Thy1 (*A*), and CD105 versus 6C3 (*B*). (Green dots are 6C3+ events, blue are Thy1+, and purple are all other events.) Expression of 6C3 (*B*) in populations that differentially express Thy1 (*A*) is indicated by linked boxes. (*C–F*) Micrographs showing osteogenic differentiation of 2,000 skeletal cells with indicated surface phenotypes after subcapsular renal transplantation (pentachrome stain). The black arrow indicates a marrow cavity. [Scale bar (*E* and *F*), 100 μm.] (*G–I*) In vitro clonal analysis of CD105(+)Thy(−)6C3(−)BCSPs. (*G*) Representative CD105(+)Thy(−) clones; the forked arrowhead indicates a chondrocyte cluster and the solid arrow indicates an osteoblast cluster. (Scale bar, 100 μm.) (*H*) Anti-Col2 immunostaining and higher magnification of the cell aggregate indicated by the forked arrowhead in *G*; positive cells (green) have a cuboidal chondrocyte morphology. (Scale bar, 500 μm.) (*I*) Osteocalcin immunostaining and higher magnification of the aggregate indicated by the solid arrowhead in *G* shows positive cells (red) with fibroblast morphology. (*Bottom* and *J–O*) In vivo clonal analysis of CD105(+)Thy(−)6C3(−) BCSPs. (*Bottom*) Schematic of the in vivo single cell skeletal progenitor transplant assay. (Scale bar, 100 μm.) (*J*) An epifluorescent stereomicroscope image showing ectopic bone under the renal capsule 1 mo after transplantation of a single GFP+ transgenic BCSP with 5,000 non-GFP fetal bone cells. The forked arrowhead points to a chondrogenic cluster (green); the solid arrowhead points to scattered osteoblasts in peripheral regions of the graft (green); the dotted yellow line delineates the cortical bone area in *J, K, M*, and *N*. (Scale bar, 100 μm.) (*K*) A representative section of the graft displayed in *J*, showing osteoblasts (solid arrowhead) in the cortical bone area. (Scale bar, 100 μm.) (*L*) A high-power image of a section adjacent to that in *K* after immunostaining with anti-osteocalcin antibody. Upper arrow points to a GFP(−) osteocalcin(+) individual osteocyte in cortical bone (red). Lower arrow points to GFP(+), osteocalcin(+) osteocyte (yellow). (*M*) A representative section of the graft displayed in *G* showing GFP-labeled stromal cells (arrowheads). (Scale bar, 20 μm.) (*N*) A different representative section of the graft displayed in *G* showing a chondrocyte cluster (forked arrowheads). (Scale bar, 20 μm.) (*O*) A high-power image of a section adjacent to that in *K* after immunostaining with anti-collagen-2 antibody shows GFP(+), collagen2(+) chondrocytes (green and yellow). (Scale bar, 20 μm.)
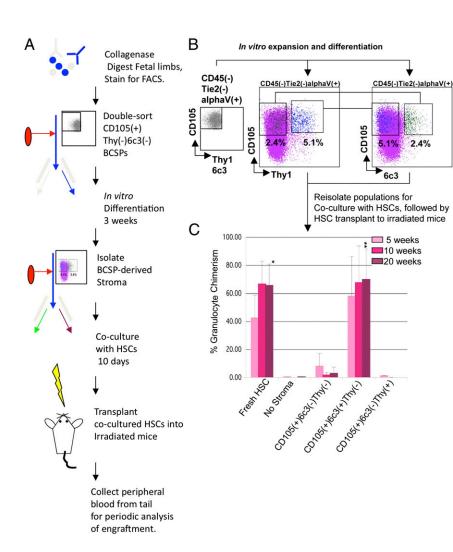
Fig. 3. A BCSP-derived CD105(+)Thy(−)6C3(+) osteogenic stromal population possesses functional HSC niche activity. (*A*) Diagram of experimental scheme. (*B*) 200,000 CD45(−)Tie2(−)CD51(+)CD105(+)Thy(−)6C3(−) BCSPs were sorted (*Left*) from limb bones and allowed to expand and differentiate in vitro for 21 d. Then (*Center* and *Right*), CD105(+) Thy1(+) (blue dots) and CD105(+)6C3(+) (green dots) were reisolated and plated with 250 freshly isolated HSCs in serum-free media containing SCF, thrombopoietin (TPO), insulin-like growth factor 1 (IGF1), and fibroblast growth factor 2 (FGF2) (purple dots are neither Thy1+ nor 6C3+). After 10 d, the cocultures were transplanted into lethally irradiated congenic recipients. Donor granulocyte chimerism was measured in the peripheral blood 5, 10, and 20 wk after transplantation. (*C*) Three mice were analyzed per group, and the results were averaged. Freshly sorted HSCs were transplanted for comparison. Only HSCs cocultured with CD105(+)6C3(+) stroma gave levels of engraftment comparable to the fresh HSC transplants. *$P < 0.05$ by ANOVA; **$P < 0.0001$ by ANOVA.

progressive stages of development (fetal, newborn, and adult) indicated that CD105 is an early marker of skeletal lineage commitment and is detectable as early as embryonic stage 13 (E13) days post coitus (dpc) in mice. In contrast, Thy1 is expressed later, at E15, during the onset of osteogenesis. Finally, 6C3 appears at E17, corresponding to the transition of fetal liver/spleen hematopoiesis to bone marrow hematopoiesis (*SI Appendix,* Fig. S3) (20, 21).
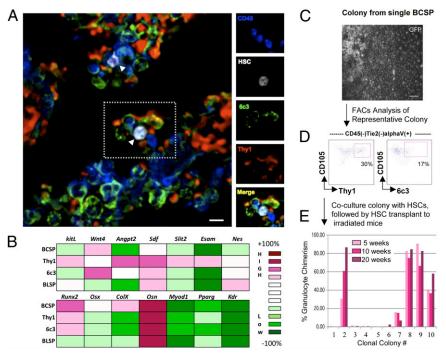
On the basis of these observations, we then fractionated CD45-Tie2-alphaV+ skeletal progenitors by differential expression of CD105, Thy1, and 6C3 and transplanted individual subsets under the renal capsule to evaluate their potential for in vivo differentiation (Fig. 2 *A–F*). GFP-labeled Thy1+ and 6C3+ cells universally formed ectopic bones 1 mo after implantation, indicating that they are restricted to osteogenic lineages. Immunostaining of the perivascular and stromal components of adult bone marrow also demonstrated the presence of Thy1+ and 6C3+ subpopulations, suggesting these cells play a role in maintenance of adult skeletal tissue (*SI Appendix,* Fig. S4). Notably, both Thy1+ and 6C3+ subsets, when transplanted, could only form bones without marrow cavities (Fig. 2 *D–F*). In contrast, the CD105+Thy1−6C3− subset could initiate formation of ectopic bones with marrow cavities containing functional HSCs, via endochondral ossification (bone formation through a cartilaginous intermediate) (Fig. 2*C*). The ectopic bones formed by CD105+Thy1−6C3− progenitors also contained Thy1+ and 6C3+ subsets (Fig. 2*C* and *SI Appendix,* Fig. S5). These findings indicate that bone, chondrocytes, and multiple

types of osteogenic stroma are all commonly derived from CD105+Thy1−6C3− skeletal progenitors (22, 23).

To determine whether the CD105+Thy1−6C3− bone, cartilage, stromal progenitor (BCSP) subset is a heterogeneous population of separate chondrocyte-restricted and osteogenic-restricted progenitors, we assayed the differentiation potential of single BCSPs. Our data indicate that single BCSPs are multipotent and capable, at the single-cell level, of generating in vitro colonies containing collagen type 2-expressing chondrocytes and osteocalcin-expressing osteoblasts (Fig. 2 *G–I*). The multipotency of BCSPs is also evident in vivo when single GFP-labeled BCSPs are transplanted with 5,000 unsorted non-GFP skeletal progenitors as supportive feeders (Fig. 2, *Bottom*). BCSPs transplanted in this fashion formed ectopic bones containing regions in which BCSP-derived cells differentiated into chondrocytes, osteoblasts, and stromal cells (Fig. 2 *J–O*). These data support the conclusion that the BCSP is the developmental branch point at which commitment to chondrocyte, bone, or stromal fates is determined.

With the BCSP as our starting point, we tested the hypothesis that the mechanisms through which the BCSP initiates niche formation also include generation of hematopoietic supportive stromal cells. There has been much speculation as to the nature and origin of hematopoietic supportive stroma. Several bone marrow-derived stromal lines such as OP9, S17, and AC6.21 can support in vitro maintenance and differentiation of hematopoietic progenitors. Of these, AC6.21 is uniquely capable of supporting both early myeloerythropoiesis and long-term

Fig. 4. Evidence that different types of osteogenic stroma act cooperatively to generate diversity in hematopoietic progenitor niches. (*A*) Newly transplanted HSC homes to 6C3(+) and Thy1(+) stroma in situ. Merged immunofluorescent image showing 6C3(+) stroma (green) and Thy1(+) stroma (red) in a cross-section of a femur from a mouse that received a transplant of RFP-labeled HSCs (white; arrowheads). The side panels show individual stains for CD45 (blue), HSCs (white), 6C3 (green), and Thy1 (red) for the region in the dotted box in *A*. (*B*) A heat map of select gene expression by microarray analysis in skeletogenic stromal populations. Skeletogenic populations are in rows and genes are in columns; the color code for expression levels is to the right. The top heat map indicates absolute expression of select genes implicated in HSC maintenance. The bottom heat map indicates absolute expression of select genes involved in osteogenesis; expression of genes involved in myogenesis (Myod1), adipogenesis (Pparg) and vasculargenesis (Kdr) are shown for comparison. (*C*) A single bone, cartilage, stromal progenitor (BCSP) generates stromal colonies that support HSCs. PI(−)CD45(−)Tie2(−)CD51(+) CD105(+)Thy(−)6C3(−) cells were single-cell sorted from limb bones and allowed to differentiate for 21 d in vitro. A brightfield image of a representative multipotent colony with a chondrocyte cluster, fibroblastic osteoblasts, and stromal cells. (Scale bar, 100 nm.) (*D*) FACS analysis of a representative multipotent colony that is capable of supporting HSCs. The presence of Thy(+) and 6C3(+) populations is indicated in the boxed region of the respective FACS plots. (*E*) 400 freshly isolated Lin(−)Ckit(+)Sca1(+)CD34(−)Slamf1(+) cells were added to the single cell-derived colonies and cultured for 10 d in serum-free media containing SCF, TPO, IGF1, and FGF2. After 10 d, 10 of the cocultured colonies were transplanted into lethally irradiated congenic recipients. At 5, 10, and 20 wk, the donor granulocyte chimerism was measured in the peripheral blood of each recipient.

lymphopoiesis, suggesting it may be capable of supporting multipotent hematopoietic stem/progenitors such as HSCs (24–26). Indeed, a derivative of AC6.21 appears to be capable of supporting expansion of human HSCs in vitro (26–30). Although its exact cellular origin remains unknown, the AC6.21 clonal cell-line was originally established from long-term Whitlock-Witte bone marrow cultures. It is also characterized by its expression of cell surface 6C3/BP-1 antigen, an aminopeptidase expressed by early B-cell progenitors and mouse B-cell lymphomas (31–33) (*SI Appendix*, Fig. S3). Because we have also observed a BCSP-derived stromal subset that is 6C3+, we tested the ability of distinct 6C3+ and Thy1+ osteogenic stromal populations derived from BCSPs to support hematopoiesis (Fig. 3 *A–C*). We cultured freshly isolated BCSPs in vitro for 3 wk to allow for differentiation and then reisolated three distinct lineages based on CD105, Thy1, and 6C3 expression: CD105+Thy1−6C3− cells that likely represent self-renewing BCSPs (and thus are candidate stem cells), CD105+ Thy1−6C3+ stroma, and CD105+Thy1+6C3− osteoblast progenitors. We then cocultured each population with HSCs in serum-free conditions with the addition of four cytokines: steel factor, thrombopoietin, insulin-like growth factor, and fibroblast growth factor (34). After 10 d of coculture, we retransplanted cocultured HSCs into lethally irradiated mice to determine whether they could still functionally reconstitute multilineage hematopoiesis [Fig. 3*C* and *SI Appendix*, Figs. S6 (diagram) and S7] (35–37). We observed that 6C3+ stroma strongly promoted survival and maintenance of multilineage reconstitution by HSC, similar to AC6.2.1 cells. Indeed, the CD105+Thy1−6C3+ stromal cell was likely the source of the original AC6.2.1 line. (Ironically, we have, by reductionist approaches to bone and bone marrow formation, apparently rediscovered the clonal stromal cell originally isolated by us in the mid-1980s.) In contrast, there was little or no engraftment by HSCs cultured without stroma under these minimal conditions. We also observed comparatively low engraftment by Thy1+ cells, indicating that 6C3+ stroma are uniquely capable of maintaining HSCs and therefore possess functional HSC niche activity at least in vitro (Fig. 3*C* and *SI Appendix*, Fig. S7). On the basis of our data, engineering combinations of 6C3+ stroma, cytokines, and possibly stromal cells of other tissue origins such as endothelium could be the key to long-term in vitro maintenance and/or expansion of HSCs.

We next explored the mechanisms by which 6C3+ stroma affect the endogenous HSC niche. To determine whether direct interaction with 6C3+ stroma facilitates HSC engraftment, we transplanted RFP-labeled HSCs and studied their association with stromal cells in situ by immunofluorescence (additional details in *Materials and Methods*). Nearly all detected HSCs were within one-cell distance of 6C3+ expressing stroma (Fig. 4*A* and *SI Appendix*, Fig. S8). Surprisingly, these HSC were also simultaneously associated with Thy1+ stroma, suggesting that HSC niches are multicellular entities composed of distinct types of hematopoiesis supporting stromal cells. Because other stromal cell types, including nestin-expressing cells, have recently been reported to associate with HSCs in the bone marrow, we conducted further immunofluorescent microscopy experiments to determine the location of 6C3+ and Thy1+ stroma relative to nestin-expressing cells. Contrary to our expectations, both 6C3+ and Thy1+ stroma expressed nestin (*SI Appendix*, Fig. S9–S11). In fact, nestin did not appear to be a specific marker for stromal cells, as we observed that nestin expression spans many types of tissues, both mature and immature, in bone marrow and other tissues (*SI Appendix*, Fig. S12) (38–43).

To understand the genetic mechanisms underlying niche function and formation, we conducted mRNA gene expression analysis on highly purified BCSP and BCSP-derived 6C3+ and Thy1+ stroma (Fig. 4*B*). In agreement with our extraskeletal transplantation studies, we found that although each of these populations expresses high levels of osteonectin (a bone lineage-associated marker), transcripts of other mesenchymal lineages such as muscle, endothelium, and adipose tissue were not detected.
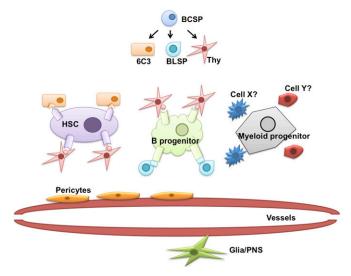
Fig. 5. Assembly of diverse niches by selective combination of BCSP-derived skeletal stroma. Proposed model of niche generation involving combinations of BCSP-derived skeletal stromal subtypes. BCSP is the progenitor of distinct stromal variants including Thy+ and 6C3 + stroma, which collectively expresses distinct repertoires of cytokines necessary for support of HSCs and HSC-derived hematopoietic progenitors. BCSP-derived stroma likely act in concert with other bone marrow populations including cells of hematopoietic, vasculature, and even glial origins to regulate hematopoiesis at the niche level.

These data suggest that the skeletal-lineage commitment of BCSP, 6C3+, and Thy1+ cells is already primed and regulated at the transcriptional level. The BCSP populations also express very high levels of the master regulator genes osterix and runt-related transcription factor 2 (runx2), which are possibly portions of the transcriptional machinery necessary for specifying skeletal and stromal fates. In addition, it is the Thy1+ subset that expresses many of the known cytokines and adhesion proteins involved in engraftment and maintenance of hematopoietic progenitors, including stem cell (steel) factor (SCF), stromal derived factor, angiopoietin, endothelial cell-selective adhesion molecule (Esam), and slit homolog 2 protein (slit2) (44–48). These cytokines and membrane proteins also possess corresponding cognate receptors on HSCs.

Despite this transcriptional profile, Thy1+ stroma did not by themselves support hematopoiesis in our experiments (Fig. 3C). In contrast, the functionally supportive 6C3+ subset expressed very little of these factors, indicating that 6C3+ stromal cells expresses factors that remain unknown but are required for HSC maintenance. Because no single stromal subset expresses all of the necessary factors for maintaining HSC niches based on transcriptional profile, niches are likely composed of multiple stromal types that act in concert to support hematopoiesis. Similarly, in clonal BCSP-derived stromal colonies, only colonies that contained both Thy1+ and 6C3+ stroma could maintain HSCs in vitro (Fig. 4 C–E). Therefore, multiple HSC-supportive stromal types in the niche are derived from BCSP.

Although we focused on stromal cells and their relation to HSC maintenance, we also observed additional BCSP-derived lineages that support more committed hematopoietic progenitors (49–50). For example, an additional CD105-Thy1+6c3− stromal lineage derived from BCSPs appears to support or direct B-lymphopoiesis exclusively (*SI Appendix*, Fig. S6). This leads us to propose a model for hematopoietic niches in which supportive environments for distinct types of primitive hematopoietic progenitors, including HSCs, are composed primarily of multiple BCSP-derived stromal types (Fig. 5). Future studies on the genetic mechanisms underlying fate selection by BCSPs could reveal the cytokine

composition of molecular programs that regulate specific types of hematopoiesis through skeletogenesis (51).

We observed that the experimental formation of bone, cartilage, and bone marrow by BCSPs attracts HSCs and vasculogenesis and appears to properly regulate hematopoiesis. The similarity between these experimental processes and endogenous processes provides evidence that the generation of the marrow involves a complex set of architectural domain constructions, as in the most complex of other tissues. This realization should further enable the study of the cellular, gene expression, and cell migration events important to hematopoiesis. The formation of an HSC niche and a B lineage niche via distinct stroma may indicate that many other niche microdomains regulating granulopoiesis, monocytopoiesis, megakaryopoiesis, and erythropoiesis exist, consist of their own stroma, and are perhaps derived from the BCSP (48). In addition, the migration of HSCs from yolk sac blood islands to aorta-gonad-mesonephros to fetal liver to spleen all involve formation, and perhaps later dissolution, of nonskeletogenic hematopoietic niches. Thus, the precise definition of niche populations, their developmental origin, and their relation to the bone-containing BCSP is crucial to understanding normal and pathogenic hematopoiesis (53–56).

Materials and Methods

See *SI Appendix, Materials and Methods* for full materials and methods.

Mice. C57BL/K_a-Thy1.1-CD45.1, C57BL/K_a-Thy1.1-CD45.1 (BA), C57BL/K_a-Thy1.2-CD45.1, and C57BL/K_a-Thy1.2-CD45.1- actin GFP, and rosa26-mRFP (C57BL/6 [B6]) strains were derived and maintained in our laboratory. All animals were maintained in Stanford University Laboratory Animal Facility in accordance with Stanford Animal Care and Use Committee and National Institutes of Health guidelines.

Isolation and Transplantation of Adult and Fetal Skeletal Progenitors. Fetal skeletal elements (humerus, radius, tibia, femur, and pelvis) were dissected from C57/BL6 BA strain fetuses and digested in collagenase with DNase at 37 °C for 40 min under constant agitation. Sorted and unsorted skeletal progenitors were pelleted and resuspended in 2 mL matrigel (regular) and then injected underneath the renal capsule of 8- to 12-wk-old anesthetized mice.

HSC-Stromal Coculture and Transplant. To establish stromal populations for HSC coculture experiments, 200,000 CD105+Thy1-6C3-CD45-Tie2-alphaV+ BCSPs were fresh-sorted from dissociated bone and bone marrow stroma of e15.5 dpc, e17.5 dpc, or newborn (postnatal day 0–3) mice and plated on 0.1% (vol/vol) gelatin-coated 15-cm culture dish and supported with MEMalpha medium supplemented with 20% FCS and PenStrep (Invitrogen) antibiotic. Two weeks after culture, cells were lifted by incubating with M199 medium supplemented with Collagenase II at 1 mg/mL and then stained and FACs-sorted for indicated populations. Then 250 fresh-sorted HSCs were added to the stromal cells and cocultured in StemPro serum-free stem cell culture media supplemented with 10 ng/mL mouse recombinant steel factor (Peprotech), 5 ng/mL mouse recombinant Thrombopoietin (Peprotech), 20 ng/mL basic fibroblast growth factor (R&D), and 25 ng/mL insulin growth factor (R&D). Culture medium was changed by removing and replacing half of it with fresh medium every other day for 10 d. On the tenth day, cells were removed for analysis and or transplanted to irradiated mice. For HSC transplants, the contents of each well corresponding to ~250 plated HSCs were combined with 300,000 unsorted host bone marrow cells as helper marrow and injected retro-orbitally into lethally irradiated (800 rad) congenic mice. Engraftment was assessed by FACS analysis of tail blood samples collected at 5-, 10-, and 15-wk intervals for analysis of expression of congenic CD45.1 or CD45.2 and blood lineage–specific markers (i.e., B-cell (B220+CD3−), T-cell (CD3+B220−), and granulocyte [B220-CD3-Gr1hi-ssc(hi)] markers).

Microarray Analyses of BM Stromal Progenitors. We performed microarrays on BCSPs, Thy1+ cells, 6C3+ cells, and B-cell lymphocyte stimulating populations (BLSPs). Each population was sorted in three independent sorts from limbs from 3- to 5-d-old male neonates. RNA was isolated with RNeasy Micro Kit (Qiagen) per manufacturer's instructions. mRNA amplification was performed using a two-cycle target labeling system for 3′ in vitro transcription, hybridized to a mouse genome 430 2.0 array, and scanned according to the manufacturer's protocol (Affymetrix). Background correction and signal normalization was performed using the standard multichip average algorithm (54–55).

CELL BIOLOGY

1. Moore KA, Lemischka IR (2006) Stem cells and their niches. *Science* 311(5769): 1880–1885.
2. Ehninger A, Trumpp A (2011) The bone marrow stem cell niche grows up: Mesenchymal stem cells and macrophages move in. *J Exp Med* 208(3):421–428.
3. Calvi LM, et al. (2003) Osteoblastic cells regulate the haematopoietic stem cell niche. *Nature* 425(6960):841–846.
4. Sacchetti B, et al. (2007) Self-renewing osteoprogenitors in bone marrow sinusoids can organize a hematopoietic microenvironment. *Cell* 131(2):324–336.
5. Yamazaki S, et al. (2011) Nonmyelinating Schwann cells maintain hematopoietic stem cell hibernation in the bone marrow niche. *Cell* 147(5):1146–1158.
6. Zhang J, et al. (2003) Identification of the haematopoietic stem cell niche and control of the niche size. *Nature* 425(6960):836–841.
7. Wu JY, Scadden DT, Kronenberg HM (2009) Role of the osteoblast lineage in the bone marrow hematopoietic niches. *J Bone Miner Res* 24(5):759–764.
8. Kopp HG, Hooper AT, Avecilla ST, Rafii S (2009) Functional heterogeneity of the bone marrow vascular niche. *Ann N Y Acad Sci* 1176:47–54.
9. Kiel MJ, et al. (2005) SLAM family receptors distinguish hematopoietic stem and progenitor cells and reveal endothelial niches for stem cells. *Cell* 121(7):1109–1121.
10. Kiel MJ, Morrison SJ (2008) Uncertainty in the niches that maintain haematopoietic stem cells. *Nat Rev Immunol* 8(4):290–301.
11. DiMascio L, Voermans C, Uqoezwa M, Duncan A, Lu D, Wu J, Sankar U, Reya T. (2007) Identification of adiponectin as a novel hemopoietic stem cell growth factor. *J Immunol* 178(6):3511–3520.
12. Naveiras O, et al. (2009) Bone-marrow adipocytes as negative regulators of the haematopoietic microenvironment. *Nature* 460(7252):259–263.
13. Méndez-Ferrer S, et al. (2010) Mesenchymal and haematopoietic stem cells form a unique bone marrow niche. *Nature* 466(7308):829–834.
14. Bhattacharya D, et al. (2009) Niche recycling through division-independent egress of hematopoietic stem cells. *J Exp Med* 206(12):2837–2850.
15. Wright DE, Wagers AJ, Gulati AP, Johnson FL, Weissman IL (2001) Physiological migration of hematopoietic stem and progenitor cells. *Science* 294(5548):1933–1936.
16. Chan CK, et al. (2009) Endochondral ossification is required for haematopoietic stem-cell niche formation. *Nature* 457(7228):490–494.
17. Sweeney E, Campbell M, Watkins K, Hunter CA, Jacenko O (2008) Altered endochondral ossification in collagen X mouse models leads to impaired immune responses. *Dev Dyn* 237(10):2693–2704.
18. Perin EC, et al. (2011) A randomized study of transendocardial injection of autologous bone marrow mononuclear cells and cell function analysis in ischemic heart failure (FOCUS-HF). *Am Heart J* 161(6):1078–1087, e3.
19. Zeller R, López-Ríos J, Zuniga A (2009) Vertebrate limb bud development: Moving towards integrative analysis of organogenesis. *Nat Rev Genet* 10(12):845–858.
20. Friedenstein AJ, Chailakhyan RK, Latsinik NV, Panasyuk AF, Keiliss-Borok IV (1974) Stromal cells responsible for transferring the microenvironment of the hemopoietic tissues. Cloning *in vitro* and retransplantation *in vivo. Transplantation* 17(4):331–340.
21. Pearse RV 2nd, Scherz PJ, Campbell JK, Tabin CJ. (2007) A cellular lineage analysis of the chick limb bud. *Dev Biol* 310(2):388–400.
22. Christensen JL, Wright DE, Wagers AJ, Weissman IL (2004) Circulation and chemotaxis of fetal hematopoietic stem cells. *PLoS Biol* 2(3):E75.
23. Morrison SJ, Hemmati HD, Wandycz AM, Weissman IL (1995) The purification and characterization of fetal liver hematopoietic stem cells. *Proc Natl Acad Sci USA* 92(22): 10302–10306.
24. Muller-Sieburg CE, Whitlock CA, Weissman IL (1986) Isolation of two early B lymphocyte progenitors from mouse marrow: A committed pre-pre-B cell and a clonogenic Thy-1-lo hematopoietic stem cell. *Cell* 44(4):653–662.
25. Adkins B, Tidmarsh GF, Weissman IL (1988) Normal thymic cortical epithelial cells developmentally regulate the expression of a B-lineage transformation-associated antigen. *Immunogenetics* 27(3):180–186.
26. Whitlock CA, Tidmarsh GF, Muller-Sieburg C, Weissman IL (1987) Bone marrow stromal cell lines with lymphopoietic activity express high levels of a pre-B neoplasia-associated molecule. *Cell* 48(6):1009–1021.
27. Spangrude GJ, Heimfeld S, Weissman IL (1988) Purification and characterization of mouse hematopoietic stem cells. *Science* 241(4861):58–62.
28. Baum CM, Weissman IL, Tsukamoto AS, Buckle AM, Peault B (1992) Isolation of a candidate human hematopoietic stem-cell population. *Proc Natl Acad Sci USA* 89(7): 2804–2808.
29. Shih CC, et al. (2000) A secreted and LIF-mediated stromal cell-derived activity that promotes ex vivo expansion of human hematopoietic stem cells. *Blood* 95(6): 1957–1966.
30. Szilvassy SJ, et al. (1996) Leukemia inhibitory factor upregulates cytokine expression by a murine stromal cell line enabling the maintenance of highly enriched competitive repopulating stem cells. *Blood* 87(11):4618–4628.
31. Wu Q, Lahti JM, Air GM, Burrows PD, Cooper MD (1990) Molecular cloning of the murine BP-1/6C3 antigen: A member of the zinc-dependent metallopeptidase family. *Proc Natl Acad Sci USA* 87(3):993–997.
32. Wu Q, et al. (1989) The early B lineage antigen BP-1 and the transformation-associated antigen 6C3 are on the same molecule. *J Immunol* 143(10):3303–3308.
33. Sherwood PJ, Weissman IL (1990) The growth factor IL-7 induces expression of a transformation-associated antigen in normal pre-B cells. *Int Immunol* 2(5):399–406.
34. Zhang CC, et al. (2006) Angiopoietin-like proteins stimulate ex vivo expansion of hematopoietic stem cells. *Nat Med* 12(2):240–245.
35. Weissman IL, Shizuru JA (2008) The origins of the identification and isolation of hematopoietic stem cells, and their capability to induce donor-specific transplantation tolerance and treat autoimmune diseases. *Blood* 112(9):3543–3553.
36. Czechowicz A, Kraft D, Weissman IL, Bhattacharya D (2007) Efficient transplantation via antibody-based clearance of hematopoietic stem cell niches. *Science* 318(5854): 1296–1299.
37. Cao YA, et al. (2004) Shifting foci of hematopoiesis during reconstitution from single stem cells. *Proc Natl Acad Sci USA* 101(1):221–226.
38. Day K, Shefer G, Richardson JB, Enikolopov G, Yablonka-Reuveni Z. (2007) Nestin-GFP reporter expression defines the quiescent state of skeletal muscle satellite cells. *Dev Biol* 304(1):246–259.
39. Mignone JL, et al. (2007) Neural potential of a stem cell population in the hair follicle. *Cell Cycle* 6(17):2161–2170.
40. Hoffman RM (2011) Nestin-driven green fluorescent protein as an imaging marker for nascent blood vessels in mouse models of cancer. *Methods Mol Biol* 689:183–204.
41. Uchugonova A, Duong J, Zhang N, König K, Hoffman RM (2011) The bulge area is the origin of nestin-expressing pluripotent stem cells of the hair follicle. *J Cell Biochem* 112(8):2046–2050.
42. El-Helou V, et al. (2005) Resident nestin+ neural-like cells and fibers are detected in normal and damaged rat myocardium. *Hypertension* 46(5):1219–1225.
43. Mignone JL, Kukekov V, Chiang AS, Steindler D, Enikolopov G (2004) Neural stem and progenitor cells in nestin-GFP transgenic mice. *J Comp Neurol* 469(3):311–324.
44. Sugiyama T, Kohara H, Noda M, Nagasawa T. (2006) Maintenance of the hematopoietic stem cell pool by CXCL12-CXCR4 chemokine signaling in bone marrow stromal cell niches. *Immunity* 25(6):977–988.
45. Ooi AG, et al. (2009) The adhesion molecule esam1 is a novel hematopoietic stem cell marker. *Stem Cells* 27(3):653–661.
46. Yokota T, et al. (2009) The endothelial antigen ESAM marks primitive hematopoietic progenitors throughout life in mice. *Blood* 113(13):2914–2923.
47. Smith-Berdan S, et al. (2011) Robo4 cooperates with CXCR4 to specify hematopoietic stem cell localization to bone marrow niches. *Cell Stem Cell* 8(1):72–83.
48. Ding L, Saunders TL, Enikolopov G, Morrison SJ (2012) Endothelial and perivascular cells maintain haematopoietic stem cells. *Nature* 481(7382):457–462.
49. Nakamura Y, et al. (2010) Isolation and characterization of endosteal niche cell populations that regulate hematopoietic stem cells. *Blood* 116(9):1422–1432.
50. Wu JY, Purton LE, Rodda SJ, Chen M, Weinstein LS, McMahon AP, Scadden DT, Kronenberg HM. (2008) Osteoblastic regulation of B lymphopoiesis is mediated by Gs {alpha}-dependent signaling pathways. *Proc Natl Acad Sci U S A* 105(44):16976–16981.
51. Weissman IL (1994) Developmental switches in the immune system. *Cell* 76(2): 207–218.
52. Muzumdar MD, Tasic B, Miyamichi K, Li L, Luo L. (2007) A global double-fluorescent Cre reporter mouse. *Genesis* 45(9):593–605.
53. Lo Celso C, et al. (2009) Live-animal tracking of individual haematopoietic stem/progenitor cells in their niche. *Nature* 457(7225):92–96.
54. Sahoo D, et al. (2010) MiDReG: A method of mining developmentally regulated genes using Boolean implications. *Proc Natl Acad Sci USA* 107(13):5732–5737.
55. Inlay MA, et al. (2009) Ly6d marks the earliest stage of B-cell specification and identifies the branchpoint between B-cell and T-cell development. *Genes Dev* 23(20): 2376–2381.
56. Weissman IL, Baird S, Gardner RL, Papaioannou VE, Raschke W (1977) Normal and neoplastic maturation of T-lineage lymphocytes. *Cold Spring Harb Symp Quant Biol* 41(Pt 1):9–21.